Thin superconducting disk with field-dependent critical current: Magnetization and ac susceptibilities

D. V. Shantsev and Y. M. Galperin

Department of Physics, University of Oslo, P.O. Box 1048 Blindern, 0316 Oslo, Norway
A. F. Ioffe Physico-Technical Institute, Polytekhnicheskaya 26, St. Petersburg 194 021, Russia

T. H. Johansen*

Department of Physics, University of Oslo, P.O. Box 1048 Blindern, 0316 Oslo, Norway
(Received 12 October 1999)

Magnetization hysteresis loops and the ac susceptibility $\chi = \chi' + i\chi''$ of a superconducting thin disk are calculated in the critical-state model assuming a field-dependent critical current density $J_c(B)$. The results are obtained by solving numerically the set of coupled integral equations for the flux and current distributions [Phys. Rev. B **60**, 13 112 (1999)] for a disk placed in a perpendicular applied field B_a. From the magnetization curves the range of fields where the vertical width of the loop $\Delta M(B_a)$ relates directly to $J_c(B_a)$ is determined. The susceptibility is analyzed in the limits of small and large ac-field amplitudes B_{am}, and also as a parametric relation $\chi''(\chi')$. Comparing our results with experimental data for $\chi''(\chi')$ shows that by taking the B dependence of J_c into account the agreement improves dramatically, in particular at small $|\chi'|$ (large field amplitudes). We show that the asymptotic behavior for large B_{am} changes from $\chi' \propto B_{am}^{-3/2}$ and $\chi'' \propto B_{am}^{-1}$ for the Bean model, to $\chi' \propto B_{am}^{-3}$ and $\chi'' \propto B_{am}^{-2}$ for J_c decreasing with $|B|$ as $|B|^{-1}$ or faster. For small B_{am} the behavior can always be described by an effective Bean model with a renormalized J_c. We also find that in the $\chi''(\chi')$ plot the peak of χ'' increases in magnitude and shifts towards $\chi' = 0$ when J_c decreases with $|B|$. This allows an easy experimental discrimination between a Bean model behavior, one with $J_c(B)$, and one where flux creep is an ingredient.

I. INTRODUCTION

The critical state model (CSM) is widely accepted as a powerful tool in the analysis of magnetic properties of type-II superconductors. In the parallel geometry, i.e., for long samples such as slabs and cylinders placed in a parallel magnetic field, an extensive amount of theoretical work has already been carried out. Exact results for flux density profiles, magnetization,[1–4] ac susceptibility,[4–6] etc., have been obtained for a number of different field-dependent critical current densities. During the last years even more attention has been paid to the CSM analysis in the perpendicular geometry, i.e., for thin samples in perpendicular magnetic fields. Assuming a constant critical current (the Bean model), explicit analytical results have been obtained for a long thin strip[7,8] and a thin circular disk.[9–12] From experiments, however, it is well known that also in such samples the critical current density j_c usually depends strongly on the local flux density B. Due to the lack of a proper theory, this dependence often hinders a precise interpretation of the measured quantities.[13–17]

In the perpendicular geometry, the ac susceptibility beyond the Bean model has been calculated only by carrying out flux creep simulations[18,19] assuming a power-law current-voltage relation with a large exponent. However, quite recently an exact analytical approach was developed for the CSM analysis of a long thin strip[20] and thin circular disk.[21] In both cases a set of coupled integral equations was derived for the flux and current distributions. In the present paper we solve these equations numerically for the thin disk case, and calculate magnetization hysteresis loops as well as the complex ac susceptibility. Results for several commonly used $j_c(B)$ dependences are presented.

The paper is organized as follows. In Sec. II we give a short description of the exact solution for the disk problem. In Sec. III, magnetization hysteresis loops are calculated and the relation between the width of the loop and j_c is discussed. The results for the complex ac susceptibility are presented in Sec. IV and analyzed with emphasis on the asymptotic behavior at small and large field amplitudes. Finally, Sec. V gives the conclusions.

II. EXACT SOLUTION

Consider a thin superconducting disk of radius R and thickness d, where $d \ll R$. We assume either that $d \gg \lambda$, where λ is the London penetration depth, or, if $d < \lambda$, that $\lambda^2/d \ll R$. In the latter case the quantity λ^2/d plays a role of two-dimensional penetration depth.[22] We put the origin of the coordinates at the disk center and direct the z axis perpendicularly to the disk plane. The external magnetic field $\mathbf{B}_a$ is applied along the z axis, and the z component of the field in the plane $z = 0$ is denoted as B. The current flows in the azimuthal direction, with a sheet current denoted as $J(r) = \int_{-d/2}^{d/2} j(r,z)dz$, where j is the current density.

A. Increasing field

We begin with a situation where the external field B_a is applied to a zero-field-cooled disk. The disk then consists of an inner flux-free region, $r \lesssim a$, and of an outer region, $a < r \lesssim R$, penetrated by magnetic flux.
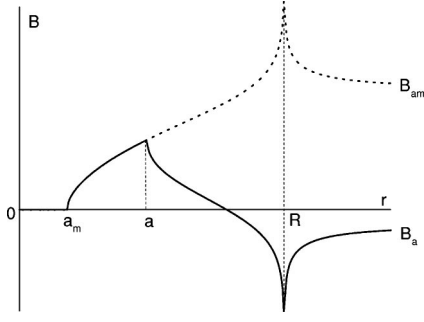
FIG. 1. Flux density profile as the applied field descends from a maximum value B_{am}.

In the CSM with a general $J_c(B)$ the current and flux density distributions in a disk are given by the following coupled equations:[21]

$$J(r) = \begin{cases} -\dfrac{2r}{\pi}\displaystyle\int_a^R dr' \sqrt{\dfrac{a^2-r^2}{r'^2-a^2}}\dfrac{J_c[B(r')]}{r'^2-r^2}, & r<a, \\ -J_c[B(r)], & a<r<R, \end{cases} \tag{1}$$

$$B(r) = B_a + \frac{\mu_0}{2\pi}\int_0^R F(r,r')J(r')dr', \tag{2}$$

$$B_a = \frac{\mu_0}{2}\int_a^R \frac{dr}{\sqrt{r^2-a^2}}J_c[B(r)]. \tag{3}$$

Here $F(r,r')=K(k)/(r+r')-E(k)/(r-r')$, where $k(r,r')=2\sqrt{rr'}/(r+r')$, while K and E are complete elliptic integrals. In the case of constant J_c, these equations reduce to the exact Bean-model formulas derived in Refs. 10 and 11.

Note that the calculation can be significantly simplified at large external field where $a \to 0$, and the critical state $J(r)=J_c[B(r)]$ is established throughout the disk. The distribution $B(r)$ is then determined by the single equation

$$B(r) = B_a - \frac{\mu_0}{2\pi}\int_0^R F(r,r')J_c[B(r')]dr', \tag{4}$$

following from Eq. (2).

B. Subsequent field descent

If B_a is reduced, after being first raised to some maximum value B_{am}, the flux density will decrease in the outer part, $a \le r \le R$, and remain trapped in the inner part, see Fig. 1. We denote the flux front position, the current density and the field distribution at the maximum field as a_m, $J_m(r)$ and $B_m(r)$, respectively. Evidently, $J_m(r)$, $B_m(r)$, and a_m satisfy Eqs. (1)–(3).

Let the field and current distributions during field descent be written as

$$B(r) = B_m(r) + \tilde{B}(r), \quad J(r) = J_m(r) + \tilde{J}(r). \tag{5}$$

The relation between $\tilde{B}(r)$ and $\tilde{J}(r)$ then reads[21]

$$\tilde{J}(r) = \begin{cases} \dfrac{2r}{\pi}\displaystyle\int_a^R dr' \sqrt{\dfrac{a^2-r^2}{r'^2-a^2}}\dfrac{\tilde{J}_c(r')}{r'^2-r^2}, & r<a, \\ \tilde{J}_c(r), & a<r<R, \end{cases} \tag{6}$$

$$\tilde{B}(r) = B_a - B_{am} + \frac{\mu_0}{2\pi}\int_0^R F(r,r')\tilde{J}(r')dr'. \tag{7}$$

$$B_a - B_{am} = -\frac{\mu_0}{2}\int_a^R \frac{\tilde{J}_c(r)}{\sqrt{r^2-a^2}}dr, \tag{8}$$

where we defined

$$\tilde{J}_c(r) = J_c[B_m(r)+\tilde{B}(r)] + J_c[B_m(r)]. \tag{9}$$

Again, setting J_c=const, these equations reproduce the Bean-model results.[10,11] If the field is decreased below $-B_{am}$ the memory of the state at B_{am} is completely erased, and the solution becomes equivalent to the virgin penetration case. If the difference $B_{am}-B_a$ is large enough then one can again use Eq. (4), only with the opposite sign in front of the integral.

Given the $J_c(B)$ dependence, a complete description of any magnetic state is now found by solving the equations numerically. An efficient iteration procedure is described in Ref. 21.

III. MAGNETIZATION

The magnetization of a disk is defined as the magnetic moment $\pi\int_0^R r^2 J(r)dr$ per unit volume. Due to symmetry the magnetization is directed along the z axis. In a fully penetrated state described by the Bean model with critical current J_{c0}, the magnetization equals $M_0=J_{c0}R/3d$. It is convenient to use M_0 for normalization, i.e.,

$$\frac{M}{M_0} = \frac{3}{R^3}\int_0^R \frac{J(r)}{J_{c0}}r^2\,dr. \tag{10}$$

The magnetization can be calculated using the current profiles obtained by the procedure described in the previous section. Shown in Fig. 2 are magnetization hysteresis loops calculated for the $J_c(B)$ dependences:

$$J_c = J_{c0}/(1+|B|/B_0) \quad \text{(Kim model)}, \tag{11}$$

$$J_c = J_{c0}\exp(-|B|/B_0) \quad \text{(exponential model)}. \tag{12}$$

A striking manifestation of the B dependence is a peak occuring at small B_a. The calculations show that for any choice of the parameter B_0, the peak is always located at *negative* B_a on the descending branch of the major loop. Such a peak position at negative B_a is a typical feature also in the parallel geometry.[1–3] However, it contrasts the case of a thin strip in perpendicular field, where it was shown analytically[23] that for any $J_c(B)$ dependence the peak is located *exactly* at $B_a=0$.

In the Bean model, there is a simple relation between the critical current and the width ΔM of the major magnetization loop
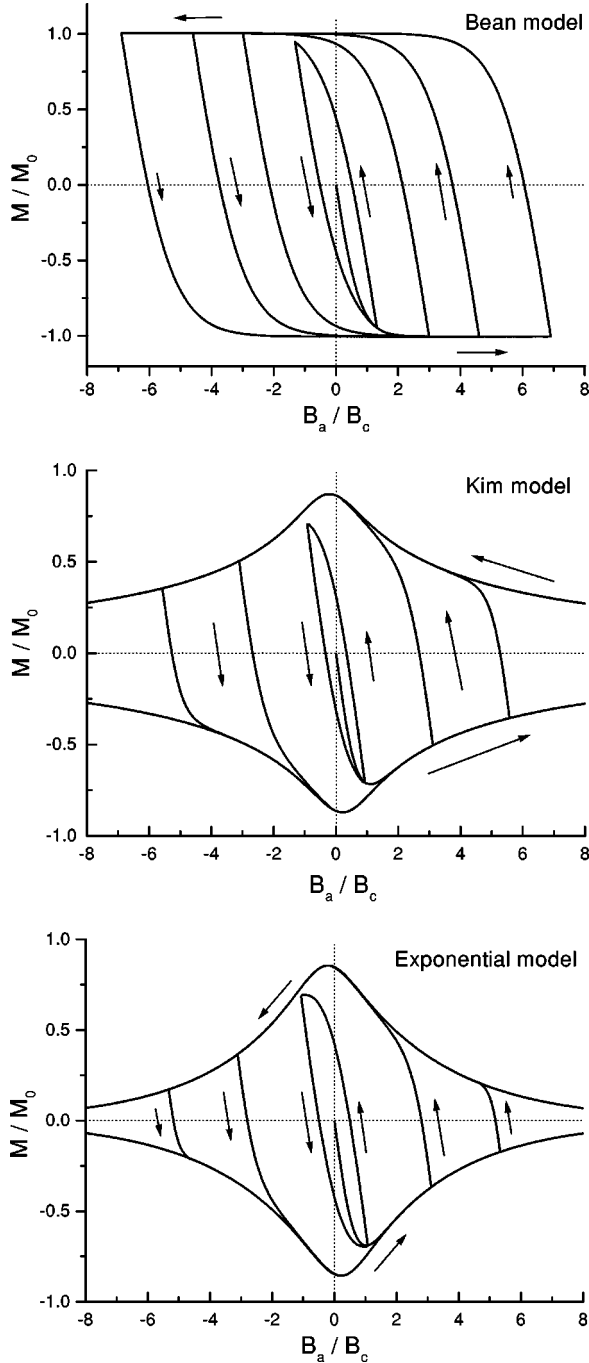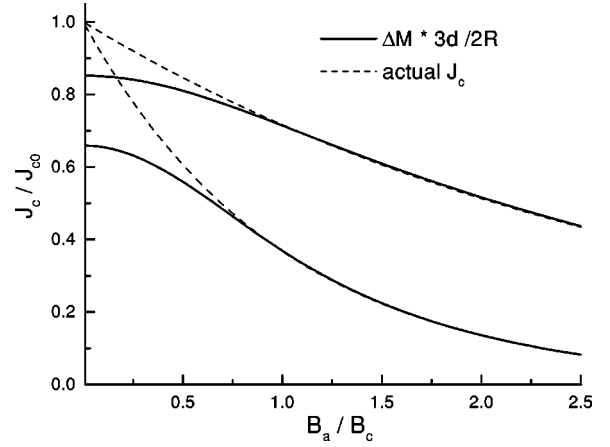
FIG. 3. The critical current inferred from the width ΔM of the major magnetization loop using Eq. (13). For comparison the plot also shows the actual $J_c(B)$ used in the calculation: the exponential model with $B_0 = B_c$ (lower curves) and $B_0 = 3B_c$ (upper curves). The agreement is excellent for fields larger than B_c.

using Eq. (13), together with the actual $J_c(B)$. One can see that at fields larger than the characteristic field

$$B_c \equiv \mu_0 J_{c0}/2, \qquad (14)$$

there is essentially no distinction between the two curves. We find that this holds independently of B_0 and also for other $J_c(B)$ models. Therefore, also for the present geometry the B dependence of J_c can be inferred directly from $\Delta M(B_a)$, except in the low-field region. Here the correct $J_c(B)$ can be obtained only by a global fit of the magnetization curve.

The Bean-model virgin magnetization for a thin disk can be expanded in B_a as[11,19]

$$-\mu_0 M \approx \chi_0 B_a \left[1 - \frac{1}{2} \left(\frac{B_a}{B_c} \right)^2 \right], \qquad (15)$$

where $\chi_0 = 8R/3\pi d$ is the Meissner state susceptibility. Our numerical calculations show that the same expansion also holds for B-dependent J_c, only with an effective value B_c^{eff} satisfying

$$B_c^{\mathrm{eff}}/B_c \approx 1 - \alpha \sqrt{B_c/B_0}. \qquad (16)$$

We find that if $B_0/B_c \gtrsim 0.5$ the parameter $\alpha = 0.50$ for the exponential model, and $\alpha = 0.43$ for the Kim model. In the parallel geometry the low-field expansion has an additional B_a^2 term which is not affected by the $J_c(B)$ dependence.[3] Thus, the deviation from the Meissner response at small B_a is there insensitive to $J_c(B)$. This result contrasts the case of perpendicular geometry where due to demagnetization effects, a B dependence of J_c affects the flux behavior even in the limit of low fields, see discussion in Ref. 21.

IV. COMPLEX ac SUSCEPTIBILITY

A. Basic expressions

The hysteretic dependence of the magnetization M as the applied field B_a is cycled leads to ac losses. The energy dissipation per cycle of B_a is

FIG. 2. Magnetization hysteresis loops for a thin disk for the Bean model ($J_c = $ const), the Kim model, Eq. (11), and the exponential model, Eq. (12), the last two both with $B_0 = 3B_c$. The parameters B_c and M_0 are defined in the text.

$$J_c = \frac{3d}{2R} \Delta M. \qquad (13)$$

The same expression is often used to determine J_c from experimental ΔM data even when the width of the observed loop is not constant. As discussed in Refs. 1–3 the applicability range of such a procedure is limited. In the parallel geometry a simple proportionality only applies for B_a larger than the full penetration field. For the thin disk case the field range where $J_c \propto \Delta M$ can be estimated from our calculations. Figure 3 shows $J_c(B)$ inferred from the magnetization loop

$$W = \int_{\text{cycle}} B_a(t) \frac{dM(t)}{dt} dt \qquad (17)$$

per unit volume. According to the critical state model, $M(t)$ follows $B_a(t)$ adiabatically, i.e., $M(t) = M[B_a(t)]$. Thus, the losses are given by the area of the magnetization hysteresis loop, $\oint M \, dB_a$.

It is conventional to express the ac response through the imaginary and real parts of the so-called nonlinear magnetic susceptibility.[13] If the applied field is oscillated harmonically with amplitude B_{am}, i.e., $B_a(t) = B_{am} \cos \omega t$, the magnetization is also oscillating with the same period. The complex susceptibility is then defined by the coefficients of the Fourier series of the in general anharmonic $M(t)$, where the real and imaginary parts are given by

$$\chi'_n = \frac{\mu_0 \omega}{\pi B_{am}} \int_0^{2\pi/\omega} M(t) \cos(n\omega t) dt,$$

$$\chi''_n = \frac{\mu_0 \omega}{\pi B_{am}} \int_0^{2\pi/\omega} M(t) \sin(n\omega t) dt,$$

respectively.

The dissipated energy, W, is determined by the response χ''_n at the fundamental frequency, namely,

$$\chi'' \equiv \chi''_1 = \frac{\mu_0 W}{\pi B_{am}^2} = \frac{2\mu_0}{\pi B_{am}^2} \int_{-B_{am}}^{B_{am}} M(B_a) dB_a. \qquad (18)$$

Below we shall also analyze the real part of the susceptibility at the fundamental frequency, $\chi' \equiv \chi'_1$, which can be expressed as

$$\chi' = -\frac{2\mu_0}{\pi B_{am}^2} \int_{-B_{am}}^{B_{am}} \frac{M(B_a) B_a dB_a}{\sqrt{B_{am}^2 - B_a^2}}. \qquad (19)$$

The $\chi''(B_{am})$ and $\chi'(B_{am})$ are calculated from these expressions using $M(B_a)$ obtained by the previously described procedure with B_{am} covering a wide range of amplitudes. For convenience, we normalize the susceptibilities to the Meissner state value $\chi_0 = 8R/3\pi d$.[11]

As seen from Fig. 4, the response χ'' shows a maximum as a function of the field amplitude. Such a maximum is in fact a common feature in all geometries. For the Bean model for a long cylinder the peak is known to occur when B_{am} is equal to the full penetration field. In the perpendicular geometry the interpretation of the peak position is not so simple. Even in the Bean model for a thin disk only numerical results are available[11]: the peak value equals $\chi''_{\text{max}} = 0.24$ and occurs at an amplitude of $B_{am} = 1.94 B_c$, corresponding to the penetration $1 - a_m/R = 72\%$. We find that the B-dependence of J_c leads to a slight increase both in a_m and in the peak magnitude. For example, the numerical results for the Kim model with $B_c = B_0$ give $\chi''_{\text{max}} = 0.29$ and $1 - a_m/R = 70\%$. The difference between various $J_c(B)$ models becomes more distinct if one analyses the asymptotic behavior at small and large field amplitudes, as shown below.
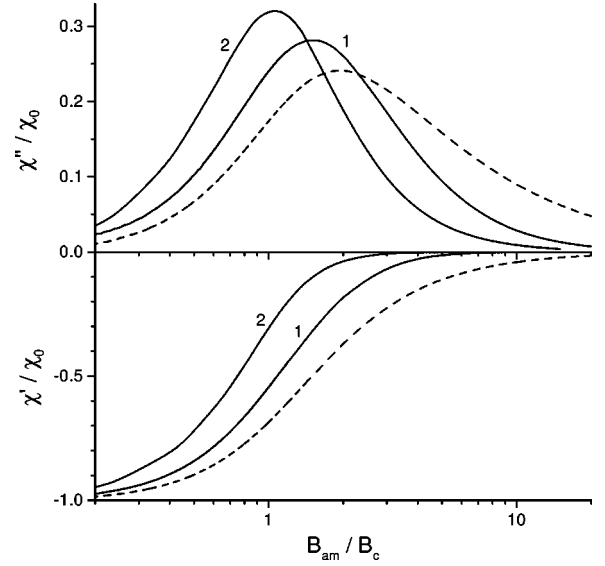

FIG. 4. Real (bottom) and imaginary (top) parts of the nonlinear susceptibility for a thin disk as functions of the amplitude B_{am} of the applied ac field. Calculations are based on Eqs. (18) and (19) with $J_c(B)$ given by the exponential model, Eq. (12), with $B_0 = 3B_c$ (curve 1) and $B_0 = B_c$ (curve 2). For comparison the results for the Bean model are also shown (dashed line).

B. Low-field behavior

At small field amplitudes the Bean model gives the exact expressions[11,19]

$$\chi'/\chi_0 = -1 + 15(B_{am}/B_c)^2/32, \qquad (20)$$

$$\chi''/\chi_0 = (B_{am}/B_c)^2/\pi. \qquad (21)$$

Shown in Fig. 5 are our numerical results for χ'' for the exponential model. From the log-log plot it is clear that the quadratic dependence on B_{am} retains as in Eq. (21) only with a modified coefficient. Moreover, we find that also χ' can be described by the Bean model expression Eq. (20) with the *same* effective B_c. The effective B_c fits the expression

$$B_c^{\text{eff}}/B_c = 1 - \alpha B_c/B_0, \qquad (22)$$

when $B_0/B_c \gtrsim 1$ with $\alpha = 0.42$ for the exponential model, and $\alpha = 0.36$ for the Kim model. Interestingly, the same ef-
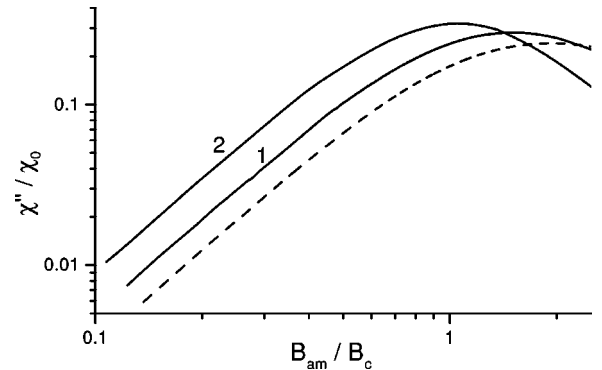

FIG. 5. Imaginary part of the susceptibility for the exponential model with $B_0/B_c = 3$ (curve 1) and with $B_0/B_c = 1$ (curve 2). At low fields both curves as well as the dashed curve presenting the Bean model result follow the same quadratic law, $\chi'' \propto B_{am}^2$.
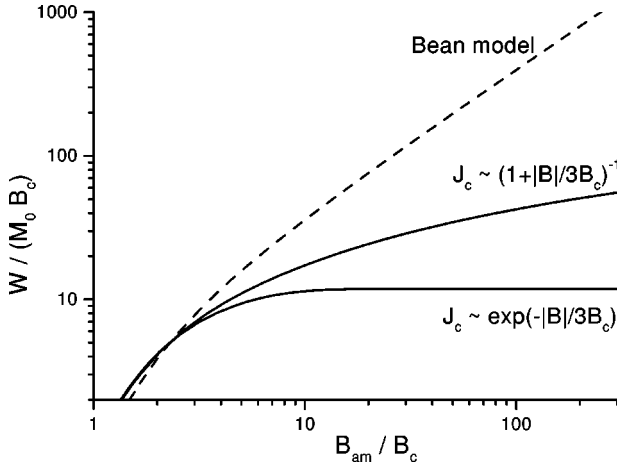
FIG. 6. High-field behavior of the dissipated energy W for the Bean, Kim, and exponential models.

fective description was found for the flux penetration depth a,[21] whereas it deviates from the description of the virgin magnetization, Eq. (16).

C. High-field behavior

The high-field behavior of the dissipated energy W is shown in Fig. 6 for a variety of $J_c(B)$ dependences. We choose to plot W rather than χ'' because the difference between the asymptotic behavior in the various models becomes more evident. One sees from the figure that for large B_{am} the Bean model yields $W \propto B_{am}$. The exponential model shows saturation, whereas one finds after a closer inspection that the Kim model leads to a logarithmic increase. These behaviors can be understood by considering the fact that for large amplitudes the disk is fully penetrated and $B(r) \approx B_a$. Therefore, $M(B_a) \propto J_c(B_a)$, and one obtains $W \propto \int^{B_{am}} J_c(B) dB$.

The high-field behavior of the real part of the susceptibility χ' for different $J_c(B)$ is shown in Fig. 7. For the Bean model we find asymptotically that $\chi'/\chi_0 = -1.33(B_{am}/B_c)^{-3/2}$ (dotted line), which is in agreement with Eq. (32) in Ref. 11. For the B-dependent J_c's we also find power-law behavior, although with different exponents. For both the Kim and exponential model the asymptotic behavior is described by $\chi' \propto B_{am}^{-3}$. However, also intermediate values for the exponent are possible, e.g., for $J_c = J_{c0}/[1 + (|B|/3B_c)^{1/2}]$ the numerical results suggest that $\chi' \propto B_{am}^{-9/4}$.

In order to understand this power-law behavior let us rewrite Eq. (19) as

$$\chi' = \frac{2}{\pi B_{am}^2} \int_0^{B_{am}} \frac{\mu_0 M_{rev}(B_a) B_a \, dB_a}{\sqrt{B_{am}^2 - B_a^2}}, \quad (23)$$

where $M_{rev} = M_\uparrow + M_\downarrow$ is the reversible magnetization. The integrand has different estimates in the regions I, II, and III indicated in Fig. 8. Therefore we divide the interval of integration correspondingly, $\chi' = \chi'_I + \chi'_{II} + \chi'_{III}$. In region I, M_{rev} does not depend on B_{am}, thus, $\chi'_I \propto B_{am}^{-3}$ at large B_{am}. In region II ($B_a \gg B_c$) we use that
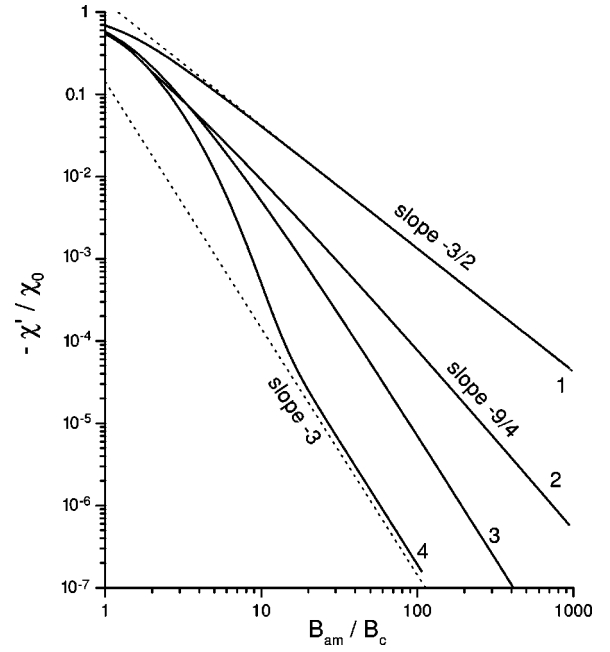

FIG. 7. High-field behavior of the real part of the susceptibility, χ', for the Bean model (curve 1) and for different $J_c(B)$ dependences; $J_c = J_{c0}/[1 + (|B|/3B_c)^{1/2}]$ (curve 2); Kim model (curve 3) and exponential model (curve 4), both with $B_0 = 3B_c$.

$$M_{rev}(B_a) \propto \int dr \, r^2 \{J_c[B_a + B_i(r)] - J_c[B_a - B_i(r)]\},$$

where B_i is the field created by the current. Expanding this expression one has $M_{rev} \propto J'_c(B_a) \int dr \, r^2 B_i(r)$. Then using the further simplification that $\int dr \, r^2 B_i(r) \propto J_c(B_a)$, one obtains

$$\chi''_{II} \propto \frac{1}{B_{am}^2} \int_{II} \frac{J_c(B_a) J'_c(B_a) B_a}{\sqrt{B_{am}^2 - B_a^2}} dB_a.$$

Taking $J_c(B) \propto (B_0/B)^s$ at large B, we arrive at the estimates, $\chi'_{II} \propto (B_c/B_{am})^2 (B_0/B_{am})^{2s}$ for small s, and $\chi'_{II} \propto (B_c/B_{am})^3 (B_0/B_c)^{2s}$ for large s. Finally, consider the region III, where $B_{am} - B_a$ is of the order of $\mu_0 J_c(B_a)$. Since the initial slope of the return branch does not depend on B_{am}, we have that $M_{rev}(B_a) \propto B_{am} - B_a$. It then follows that, $\chi'_{III} \propto (B_c/B_{am})^{3/2} (B_0/B_{am})^{3s/2}$. As the asymptotic behavior at large B_{am} is determined by the slowest decaying term, we arrive at the following result:
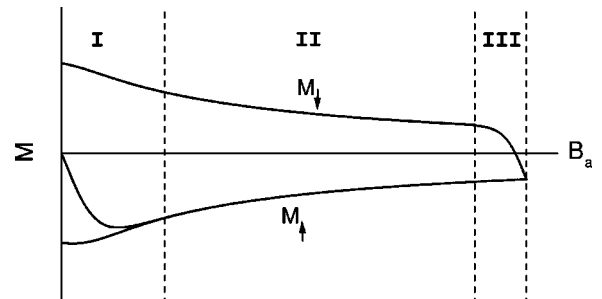

FIG. 8. Division of a magnetization loop into three regions treated differently when estimating χ' at large B_{am}.
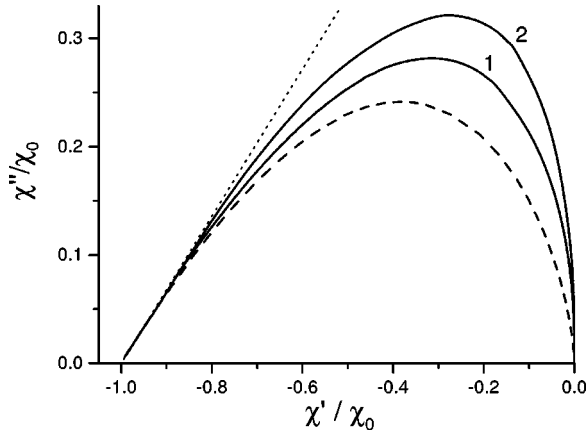
FIG. 9. Parametric plot of the complex susceptibility for a thin disk using the three sets of curves presented in Fig. 4. The dotted line shows the Bean model asymptotic behavior, Eq. (25). A B dependence of J_c substantially distorts the plot, although not the slope at $\chi' \to -1$.

$$\chi' \propto \begin{cases} B_{am}^{-3(1+s)/2}, & s<1, \\ \\ B_{am}^{-3}, & s \geq 1. \end{cases} \qquad (24)$$

These power laws fully agree with our numerical calculations shown in Fig. 7. The expression (24) gives the exact values for the exponent found for the Bean model ($s=0$), the Kim ($s=1$) and exponential ($s=\infty$) models and even for the $J_c(B)$ with $s=1/2$. Note however, that this asymptotic behavior is sometimes established only at rather low values of $|\chi'|$, see curve 4 in Fig. 7. Therefore one should be very careful in interpretation of corresponding experimental log-log plots.

It should be specially emphasized that the presented analysis for the high-field asymptotic behavior is not restricted to a thin disk. In fact, we expect the result (24) to be valid in *any geometry*. This result is also in agreement with numerical calculations for long samples described by the Kim and the exponential model.[5]

D. Plots of χ'' versus χ'

In contrast to graphs of χ as a function of the field amplitude or temperature, a plot of χ'' versus χ' contains only dimensionless quantities, and is therefore very useful for analyzing experimental data.[14,15] In practice, such a parametric plot $\chi''(\chi')$ can be obtained by scans either over the magnetic field amplitude or over the temperature. Figure 9 presents the $\chi''(\chi')$ plot of the data shown in Fig. 4. We observe that a B dependence of J_c gives a significant distortion of the graph. Compared to the Bean model one finds that: (i) the maximum is shifted to higher values of χ'', (ii) it occurs at smaller values of $-\chi'$, and (iii) in the limit of large B_{am} (or high temperatures) χ'' falls to zero more abruptly.

Meanwhile, at small B_{am}, as $\chi' \to -1$, the slope of $\chi''(\chi')$ curve remains the same as in the Bean model, namely,

$$\frac{\chi''}{\chi_0} = \frac{32}{15\pi}\left(1+\frac{\chi'}{\chi_0}\right) \quad \text{at} \quad \chi' \to -1. \qquad (25)$$
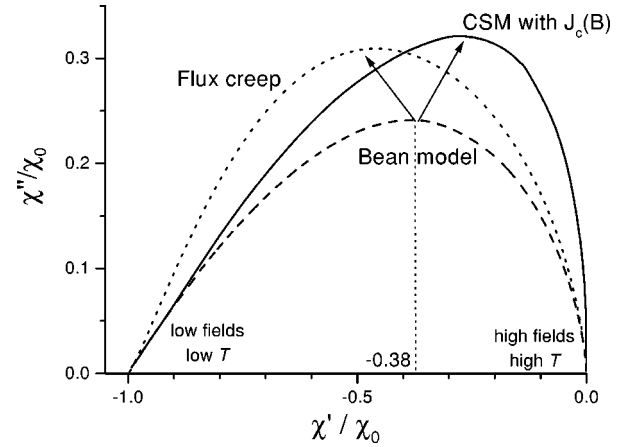

FIG. 10. The behavior of $\chi''(\chi')$ for various models. The Bean model predicts a peak located at $\chi'_{max} = -0.38$. A B dependence in J_c shifts the peak to the right and changes the behavior at $\chi' \to 0$ (our results), while flux creep shifts it to the left and changes the behavior at $\chi' \to -1$ (Ref. 19).

This result holds for *any* $J_c(B)$. It also follows from the previous analysis showing that at low fields both χ' and χ'' are modified by $J_c(B)$ in the same way. The universal slope given by Eq. (25) allows one to examine if experimental data are described by the critical state model without *a priori* knowledge of the actual $J_c(B)$ dependence for the sample.

The presented $\chi''(\chi')$ plots for a disk in a perpendicular field should be compared to similar plots for the long samples in a parallel field studied systematically in Ref. 5. As expected, the Bean-model curve for a thin disk shown by the dashed line in our Fig. 9 appears quite different from the Bean-model curves for long samples shown in Figs. 7(a), Figs. 7(b) of Ref. 5. Meanwhile, further analysis of these figures shows that the account of a B-dependent J_c always leads to very similar distortions of the $\chi''(\chi')$ plots. Namely, in all geometries the χ'' peak increases in magnitude and shifts towards $\chi'=0$. Note that such a behavior is found when the characteristic field B_0 of the $J_c(B)$-dependence is larger or of the order of B_c. For $B_0 \ll B_c$ this behavior may change qualitatively. In particular, in the parallel geometry, the peak position, χ'_{max}, becomes a nonmonotonous function of B_0.[5] However, the case of $B_0 \ll B_c$ is not very realistic for a thin disk since B_c is proportional to the sample thickness while B_0 is usually taken as geometry independent.

It is interesting to compare our $\chi''(\chi')$ plots to the ones obtained by calculations based on a nonlinear current-voltage curve $j \propto E^{1/n}$, $n < \infty$. Shown in Fig. 10 together with the CSM results is a $\chi''(\chi')$ curve (dotted line) drawn in accordance to typical graphs presented in Refs. 18,19. Compared to the Bean model curve, the maximum of χ'' increases in magnitude and shifts towards $\chi'=-1$. Moreover, the slope at $\chi' \to -1$ becomes steeper. The last two features are in a strong contrast to the effect of having a B-dependent J_c in the CSM. Consequently, an analysis of the $\chi''(\chi')$ plot allows one to discriminate between a strict CSM behavior and one where flux creep is an ingredient.

Finally, we compare in Fig. 11 our theoretical results to available experimental data on the susceptibility of YBaCuO films.[14,15,24] The shown data were obtained by reading selected points in the graphs found in the literature. It is evi-
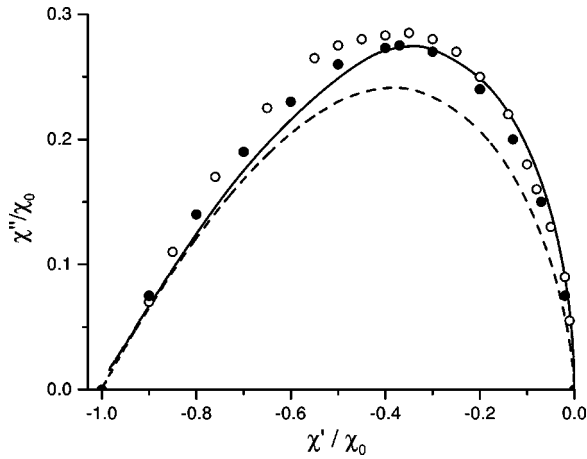
FIG. 11. Experimental susceptibility data from Ref. 14 (open circles) and Ref. 15 (solid circles) (Ref. 24) together with the CSM predictions for a thin disk: the Bean model (dashed curve) and the Kim model with $B_0=3B_c$ (full line). The Kim model gives a better agreement with experiment over the whole range.

dent that the poor fit by the Bean model (dashed curve) is greatly improved by the curve (full line) calculated for a B-dependent J_c. Whereas the agreement is better throughout the $\chi''(\chi')$ plot, it is especially evident at small $|\chi'|$ (large field amplitudes), where the $J_c(B)$ dependence plays a major role. There is still a discrepancy in the low-field region, where all experimental points do not follow the universal CSM slope given by Eq. (25). The deviation can be caused by a flux creep leading to a steeper slope.[18,19] This suggestion can be checked experimentally by analyzing $\chi''(\chi')$ plots obtained at different temperatures.

V. CONCLUSION

Magnetization and ac susceptibility of a thin superconducting disk placed in a perpendicular magnetic field were analyzed in the framework of the critical state model where J_c depends on the local flux density. We solved numerically the set of coupled integral equations for the flux and current distributions, and from that calculated magnetization hyster-

esis loops as well as the susceptibility, $\chi=\chi'+i\chi''$. The results, which were obtained for several commonly used J_c decreasing with $|B|$, allowed us to determine the range of fields where the vertical width of the major magnetization loop, $\Delta M(B_a)$, is directly related to $J_c(B_a)$.

We have shown that at small fields the virgin magnetization and complex susceptibility have the same dependence on B_a as for the Bean model, although with different coefficients. For large ac amplitudes B_{am} the behavior of the ac susceptibility changes from $\chi'\propto B_{am}^{-3/2}$ and $\chi''\propto B_{am}^{-1}$ for the Bean model, to $\chi'\propto B_{am}^{-3}$ and $\chi''\propto B_{am}^{-2}$ for J_c decreasing with $|B|$ as $|B|^{-1}$ or faster. We could show numerically, and also presented an argument, that when asymptotically $J_c\sim|B|^{-s},s<1$, one has $\chi'\propto B_{am}^{-3(1+s)/2}$. The results for the high-field behavior of the susceptibility are expected to be valid for superconductors of *any geometry*.

A most convenient test for critical-state models is provided by an analysis of the $\chi''(\chi')$ plot. We conclude that the asymptotic behavior at $\chi'\rightarrow-1$ is universal for the CSM with *any* $J_c(B)$. On the other hand, flux creep can affect this behavior. The peak in χ'' at $\chi'=-0.38$ predicted by the Bean model was found to be shifted toward $\chi'=0$ due to the B dependence in J_c, and toward $\chi'=-1$ because of flux creep.

Note added in proof. We have recently carried out independent numerical simulations to verify the conclusion about the influence of the creep on the $\chi''(\chi')$ peak position. We have found that the above conclusion is valid if the simulations are based on the nonlinear $E(j)$ curve, $E\propto(j/j_c)^n$, as in Refs. 18 and 19. However, simulations based on the classical flux diffusion approach where $E\propto B(j/j_c)^n$ show that the peak position is determined only by the $J_c(B)$ dependence and is practically insensitive to the creep. The shift of the peak due to $J_c(B)$ dependence has also been observed in Ref. 19 from numerical simulations.

ACKNOWLEDGMENTS

*Electronic address: t.h.johansen@fys.uio.no

[1] D. X. Chen and R. B. Goldfarb, J. Appl. Phys. **66**, 2489 (1989); D. X. Chen, A. Sanchez, and J. S. Minoz, *ibid.* **67**, 3430 (1990).

[2] P. Chaddah, K. V. Bhagwat, and G. Ravikumar, Physica C **159**, 570 (1989).

[3] T. H. Johansen and H. Bratsberg, J. Appl. Phys. **77**, 3945 (1995).

[4] J. R. Clem, J. Appl. Phys. **50**, 3518 (1979).

[5] D. X. Chen and A. Sanchez, J. Appl. Phys. **70**, 5463 (1991).

[6] M. Forsthuber and G. Hilscher, Phys. Rev. B **45**, 7996 (1992).

[7] E. H. Brandt and M. Indenbom, Phys. Rev. B **48**, 12 893 (1993).

[8] E. Zeldov, J. R. Clem, M. McElfresh, and M. Darwin, Phys. Rev. B **49**, 9802 (1994).

[9] P. N. Mikheenko and Yu. E. Kuzovlev, Physica C **204**, 229 (1993).

[10] J. Zhu, J. Mester, J. Lockhart, and J. Turneaure, Physica C **212**, 216 (1993).

[11] J. R. Clem and A. Sanchez, Phys. Rev. B **50**, 9355 (1994).

[12] Some final expressions obtained in Ref. 9 are not correct, see discussion in Ref. 10.

[13] F. Gömöry, Supercond. Sci. Technol. **10**, 523 (1997).

[14] O. Stoppard and D. Gugan, Physica C **241**, 375 (1995).

[15] Th. Herzog, H. A. Radovan, P. Ziemann, and E. H. Brandt, Phys. Rev. B **56**, 2871 (1997).

[16] B. J. Jönsson, K. V. Rao, S. H. Yun, and U. O. Karlsson, Phys. Rev. B **58**, 5862 (1998).

[17] B. A. Willemsen, J. S. Derov, and S. Sridhar, Phys. Rev. B **56**, 11 989 (1997).

[18] E. H. Brandt, Phys. Rev. B **55**, 14 513 (1997).

[19] E. H. Brandt, Phys. Rev. B **58**, 6523 (1998).

[20] J. McDonald and J. R. Clem, Phys. Rev. B **53**, 8643 (1996).

[21] D. V. Shantsev, Y. M. Galperin, and T. H. Johansen, Phys. Rev. B **60**, 13 112 (1999).

[22] P. G. de Gennes, *Superconductivity of Metals and Alloys* (Benjamin, New York, 1966).

[23] D. V. Shantsev, M. R. Koblischka, Y. M. Galperin, T. H. Johansen, L. Pust, and M. Jirsa, Phys. Rev. Lett. **82**, 2947 (1999).

[24] The Bean-model $\chi''(\chi')$ curves for all geometries presented in Fig. 2 of Ref. 14 and Fig. 4 of Ref. 15 are incorrect. At large field amplitudes, i.e., at $\chi' \to 0$, they show a linear behavior, while the true Bean-model behavior is always $\chi'' \propto |\chi'|^{2/3}$ [see, e.g., discussion in Ref. 19 or exact results for the disk case in Eqs. (32) and (33) of Ref. 11].